BioGecko Vol 12 Issue 02 2023

ISSN NO: 2230-5807

Modeling a Binary Organic Rankine Cycle operated with solar collectors: Case study -Ecuador

Daniel Chuquin-Vasco[1,] *, Cristina Calderón-Tapia[2] , Nelson Chuquin-Vasco[3] , Juan Chuquin-Vasco[3] and Diana Aguirre-Ruiz [4]

[1] Escuela Superior Politécnica de Chimborazo (ESPOCH), Faculty of Sciences, Safety, Environment and Engineering Research Group (GISAI); daniel.chuquin@espoch.edu.ec (D.CH.V);

[2] Escuela Superior Politécnica de Chimborazo (ESPOCH), Faculty of Sciences, Grupo de investigación Desarrollo para el ambiente y Cambio Climático (GIDAC); cristina.calderont@espoch.edu.ec (C.C.T);

[3] Escuela Superior Politécnica de Chimborazo (ESPOCH), School of Mechanics, Safety, Environment and Engineering Research Group (GISAI);nelson.chuquin@espoch.edu.ec (N.CH.V); juan.chuquin@espoch.edu.ec(J.CH.V)

[4] SOLMA, Advanced Mechanical Solutions, Mechanical Engineering and Construction Services (D.A.R);

Correspondence: daniel.chuquin@espoch.edu.ec

Abstract: The present study models a Binary Organic Cycle with solar panels, analyzing the system through the Thermal Module (parabolic solar collectors and energy storage tank) and the Organic Rankine Cycle Module (ORC). The first objective was to determine the Equator Region in which the thermal module presents the best efficiency of the solar collectors, then a detailed analysis of the ORC Module is made according to a working fluid, boiling temperature, condensation temperature, pinch point temperature, solar collector area and the ratio of collector area to the volume of the energy storage tank (Ac/V). Finally, an economic analysis is performed based on the net present value (NPV), the internal rate of return (IRR) and the payback period for implementing such a system. After performing all the respective analyses in the Thermal Module, it was determined that in the Sierra Region of Ecuador, due to its meteorological conditions (Tamb = 14.7 and Gb=184.5 watt/m2), the efficiency of the collectors is higher; this efficiency is also favored by using Therminol VP-1 as thermal fluid because it has better thermodynamic properties than the other fluids analyzed. Similarly, the ORC Module analysis results determine that Cyclohexane is the ORC working fluid that leads to a higher efficiency of the ORC (25%) and the system in general (20%). Therefore, the optimal operating conditions of the system are: solar collection area of 1600m2, energy storage tank volume of 54 m3, network output (7.42 TJ/year), the total system yields 22 %, with an IRR of 15.65 % and a payback period of 9.81 years.

Keywords: Solar collectors, working fluid, ORC, thermal module, power, energy.

1. Introduction

As the population grows, the consumption of electrical energy increases and consequently, its production from non-renewable sources such as the burning of fossil fuels, which represents a serious environmental impact problem. From this point of view, due to its geographical location, Ecuador becomes a country where solar energy can be an alternative to hydroelectric power plants, which cover 76.65% of the total electricity demand in the country, and only 0.11% corresponds to photovoltaic energy [1]. The advantage lies in the fact that, being located on the equatorial line, direct solar radiation is perpendicular all year round and only varies according to the meteorological conditions of each region of Ecuador (Coast, Highlands, East and Insular). Regarding the use of solar energy, according to the National Energy Efficiency Plan 2016 - 2035, the main objective

today is to reduce energy consumption per unit of physical production in industry subsectors using cogeneration energy systems which can be coupled with solar collectors to increase the energy efficiency of the system. It is estimated that by 2035, with these techniques, companies can reduce their energy consumption by 29.9 Mboe. Currently, only three sugar mills supply electricity from cogeneration, with a total capacity of 136.4 MW [2].

1.1. Organic Rankine Cycle

The worldwide energy demand has increased due to overpopulation, which forces governments to look for environmentally friendly alternatives by generating electricity from renewable energies and using waste heat from industrial processes. Organic Rankine systems (ORC) are power systems that have simple configurations and can operate at low temperatures and high yields by using organic substances as working fluids with low boiling points [3].

Review articles such as the ones presented by Bao & Zhao [4], Lecompte et al. [5], and Velez et al. [6] have given an overview of the cycles, the selection of the working fluid and the main components of the system. However, most existing studies have considered the technical difficulties related to the heat source only for specific case studies. The heat source is one of the most important aspects during the design and construction of an ORC since the heat source conditions are the working conditions imposed on the cycle and its thermodynamic performance. The primary heat sources used in ORCs come from waste heat from industrial processes, internal combustion machines, gas turbines, and renewable energies (solar, geothermal, biomass), and the main parameters considered for their selection are temperature, capacity, thermodynamic performance and cost [7].

The most common way to produce electricity from solar energy is by applying the basic Rankine cycle. However, when the heat source temperatures are low, around 300 C, the organic Rankine cycle - ORC [8]. In this temperature range, due to the thermal characteristics they offer, MDM (Octamethyltrisiloxane), MM (Hexamethyldisiloxane), isopentane, and Cyclohexane, among others, are generally used as working fluids. The lower critical point and the positive slope formed in the T-S diagram determine the suitability of the selected working fluid [9]. In the temperature range of 150 - 200 °C, isopentane and isobutane are generally the fluids that are used as working fluids [10,11]. [10,11]. Delgado-Torres et al. [10] conducted studies to determine the performance of different solar collectors (PTC- Parabolic trough collectors, ETC - Evacuated tube collectors, FPC - Smooth plane collectors) on the thermal efficiency of ORC in desalination systems for electricity production (0.5 MW) employing MM and R245fa as working fluids, they determined that parabolic trough collectors are the ones that led to higher performance.

1.2. ORC Thermodynamic Analysis

ORCs work with high molecular weight organic fluids with critical thermodynamic properties different from water ones and are characterized by increased heat recovery and cycle efficiency [12,13]. Figure 1 shows the main components of a basic ORC and the Temperature vs. entropy (T-s) diagram where the four ideal processes of the cycle are represented. The basic ORC consists of a pump that raises the pressure of the working fluid and transports it to the evaporator (Point 1). In the evaporator, the working fluid is heated to its saturation point or superheated steam (Point 2). The fluid then expands in the turbine, producing mechanical work (Point 3), which a generator transforms into electrical energy. Next, the superheated fluid is condensed as a saturated liquid (Point 4). Finally, the pressure in the pump is raised, thus closing the thermodynamic cycle. The heat dissipated and supplied represent a finite thermal reservoir and are represented by points 7 - 8 and 5 - 6.

The selection of the working fluid is decisive in ORC processes, and its choice depends on the application for which it will be designed. [14]. The ORC can work with saturated steam or

constantly superheated fluid. Superheating to elevated temperatures to prevent the vapor from entraining liquid droplets is unnecessary since, unlike water, it terminates its expansion in the superheated vapor area for most of the fluids used. Superheating improves the efficiency of the cycle; however, as the heat exchanger heat coefficients are low, large and expensive heat exchangers are required [15]. The technical criteria for selecting the type of fluid are thermodynamic efficiency of the cycle, net power produced, rate of return on investment, and net power produced per heat transfer area, while the thermodynamic parameters taken into consideration are critical boiling pressure and temperature, critical condensing pressure and temperature, latent heats, low freezing point, low vaporization enthalpy, and low environmental impact (Sampedro, 2017).

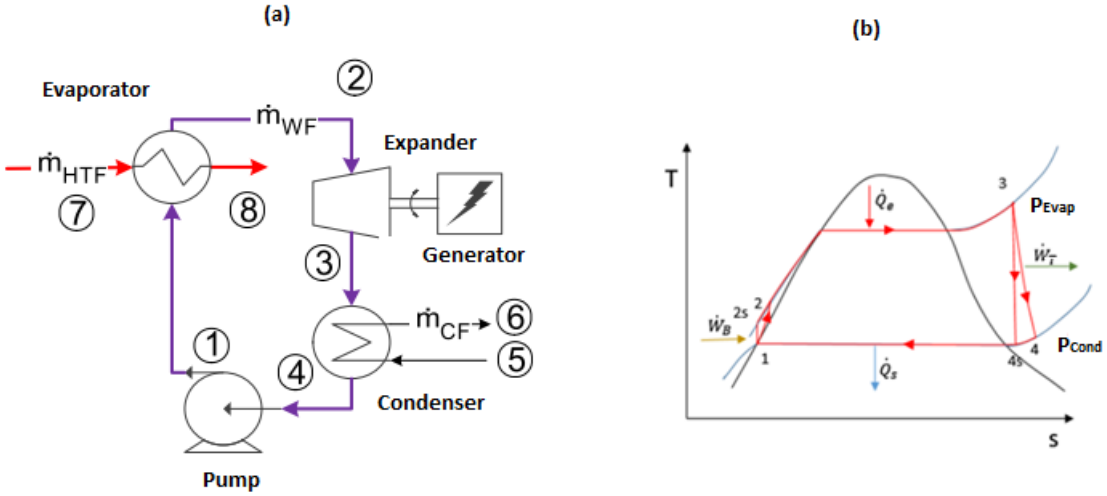

Figure 1. (a) Main components of an ORC, (b) T vs. s diagram of an ORC.
Source: [5]

1.2. Heat Source in ORCs

Depending on the configuration, power and temperature of the heat source, ORC can take advantage of different types of available energy, such as industrial waste heat, geothermal, solar, exhaust gases, and nuclear energy [6] [7]. Therefore, the categorization of the heat sources is important to take into account for the optimization of the thermodynamic cycle and the selection of the working fluid. Table 1 details the typical characteristics of the heat sources used in the ORC.

Generally, solar collectors operated at elevated temperatures provide the ORC with good efficiencies; however, collector efficiency decreases, and solar panel implementation costs increase. For this reason, every system designed has an optimum design temperature [16]. The energy storage in solar collectors depends on the fluctuation in solar radiation levels; several studies employed dynamic models to evaluate the effects of radiation on electric power generation as a function of weather conditions [17-19]. In ORCs operated with solar collectors, radiation is stored as energy in reservoirs installed between the collectors and the ORC in such a way that the efficiency of the system is maintained, and usually have three (3) modes of operation: solar mode during periods of low insolation, solar with energy storage during periods of high insolation, and release of the stored energy at night [20].

Table 1. Heat source characteristics

Heat Source	*Temperature*	*Medium*	*Capacity*	*System Cost*	*References*

Industrial	*80 - 500 C*	*Water, air or steam*	*125 kW - 3 MW*	*1800 - $5500 /kW.*	[21,22]
Residual Heat	*80 - 100 C (Cooling system). 400 - 900 C (Exhaust gases).*	*Water or oil with other gases*	*95 kW - 6.5 MW.*	-	[23-25]
Geothermal	*80 - 180 C*	*Water with brine*	*0.6 - 27 MW*	*$1500 - $5000*	[26,27]
Solar Collector	*< 300 C*	*Water or oil*	*< 30 MW*	*MW system $6000 - $7500 /kW*	[28]
Biomass	*Approximately 300 C*	*Oil*	*100 - 1500 kW*	*2,000/kW at medium scale. $12000/kW large scale*	[29-31]

2. Materials and Methods

This study will model an organic Rankine cycle (ORC Module) using solar collectors (Thermal Module) and waste heat as a heat source. The model is developed to determine the optimal design parameters that maximize the thermal performance of the ORC while minimizing the solar energy collection area.

Figure 2 shows the methodological scheme for developing and evaluating the developed model. First, a thermodynamic analysis of the thermodynamic oil used in the Thermal Module and the working fluids of the ORC Module was carried out based on the operating conditions imposed by the system. Subsequently, an energy evaluation was carried out to determine an optimal solution, maximizing the internal rate of return (IRR). The parameters to be optimized were: the solar collector area of the panels, the energy storage tank volume and the system's installation costs.

2.1. System Description

Figure 3 shows the schematic of the modeled system, which consists of 2 modules: The Thermal Module and the ORC Module (With a recuperator). The Thermal Module comprises a set of Solar Collectors operated with thermal oil and an Energy Storage Tank, which can transfer the heat to the ORC Module through the heat exchanger. While the ORC Module is composed of 4 equipment (Pump, Heat Exchanger, Turbine, Recuperator, and Condenser) in which 4 processes take place. In Process 1 - 2, a compression process takes place; the fluid, as a saturated liquid at low pressure, enters the pump to reach the maximum pressure of the cycle. In Processes 2-3 and 5-6, the fluid is internally heated by heat exchange (Recuperator) with the saturated steam coming from the turbine to increase the total energy efficiency of the cycle. In Processes 3 - 4, a heat transfer (Exchanger) between the Thermal Module Oil and the ORC working fluid results in superheated steam at point 4. In Processes 4 - 5, the superheated steam expands in the turbine up to the minimum cycle pressure, transforming the working fluid into saturated steam (Point 5). Finally, in Process 6-1, the saturated steam is converted into saturated liquid in the condenser (Heat Rejection) to start the cycle again.

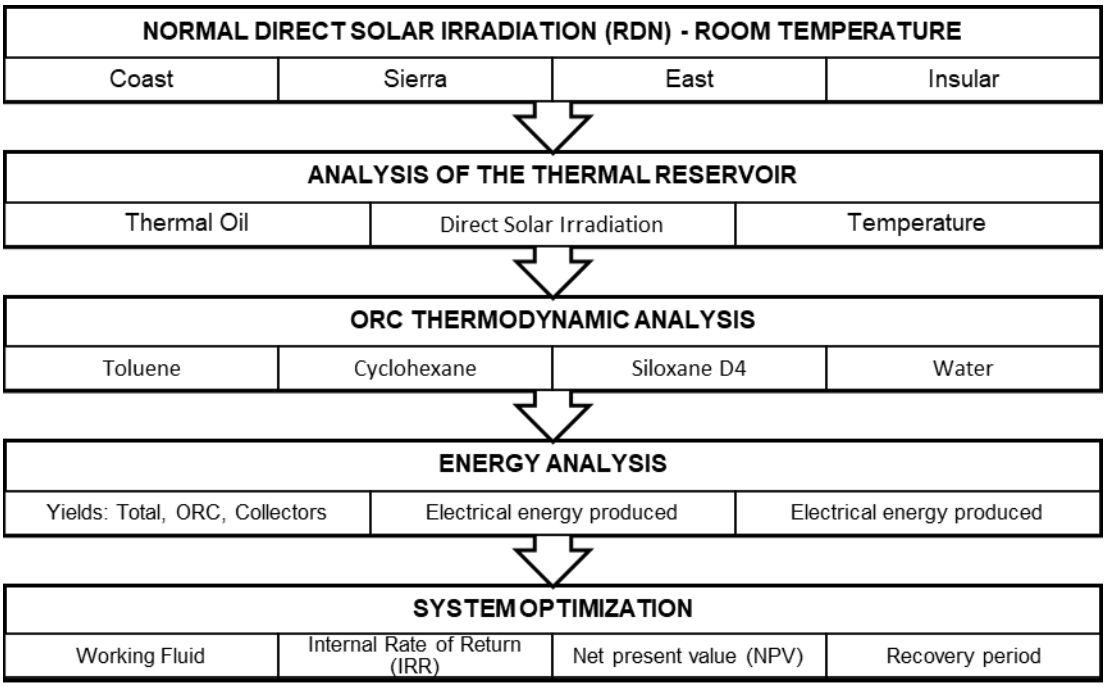

Figure 2. Methodology for system modeling

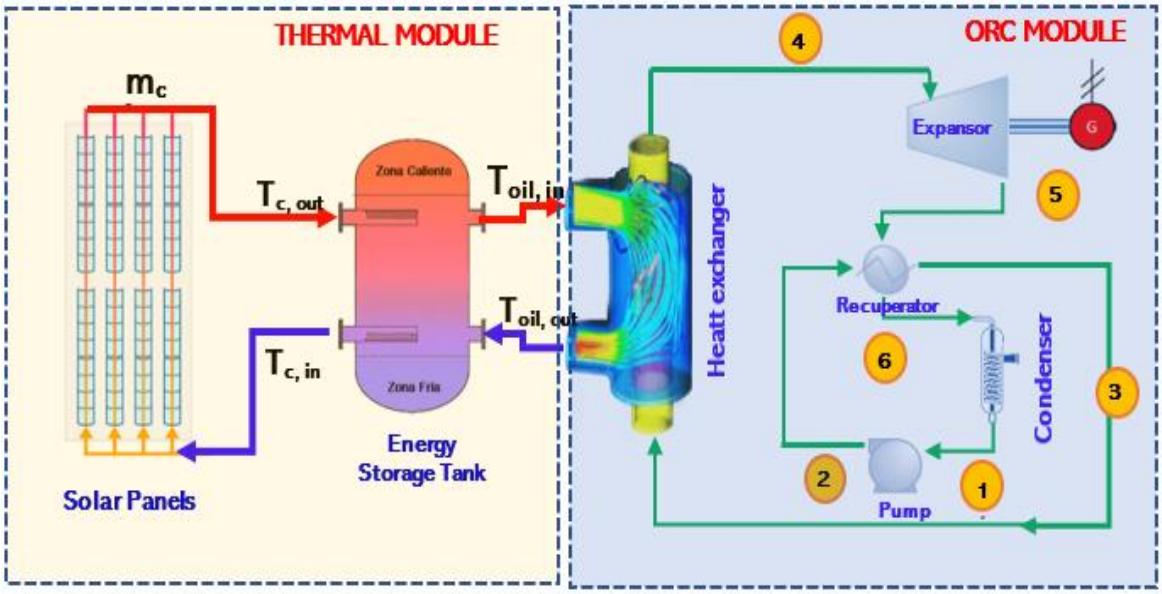

Figure 3. Schematic representation of the developed model

2.2. Modeling Parameters

The meteorological data for the modeling were taken from the National Renewable Energy Laboratory (NREL) website. The four regions of Ecuador were considered for the analysis since the typical temperature throughout the year varies in each of them (Coast, Highlands, East and Insular (Galapagos). Figure 4 shows the ambient temperature for each of the regions of Ecuador, while Figure 5 details the values of solar irradiation received by the collector depending on the region where it is located. It is important to note that only direct normal irradiation can be used by parabolic trough collectors since they only absorb a specific solar image. In Table 2, the conditions

assumed for the system modeling are detailed. These values have been reasonably selected based on actual operating conditions and have been tested in preliminary studies [32].

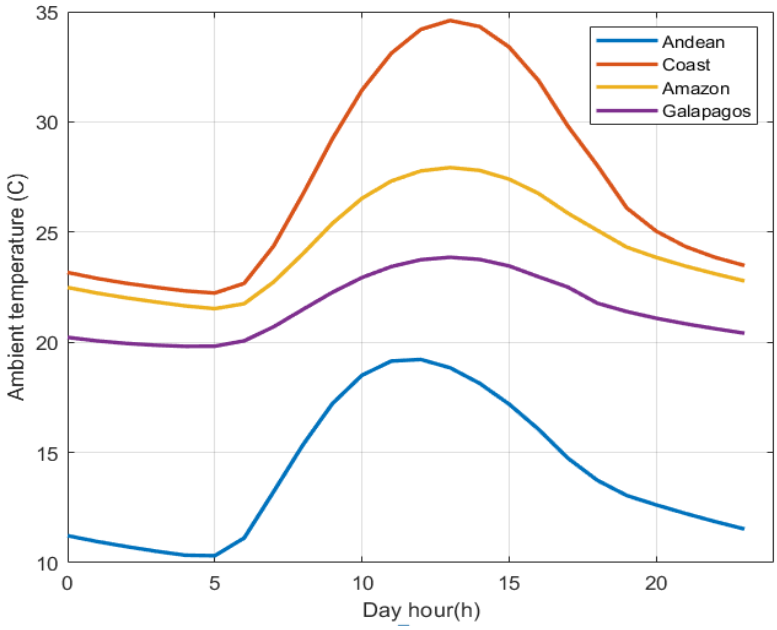

Figure 4. Ambient temperature (Equator Regions)

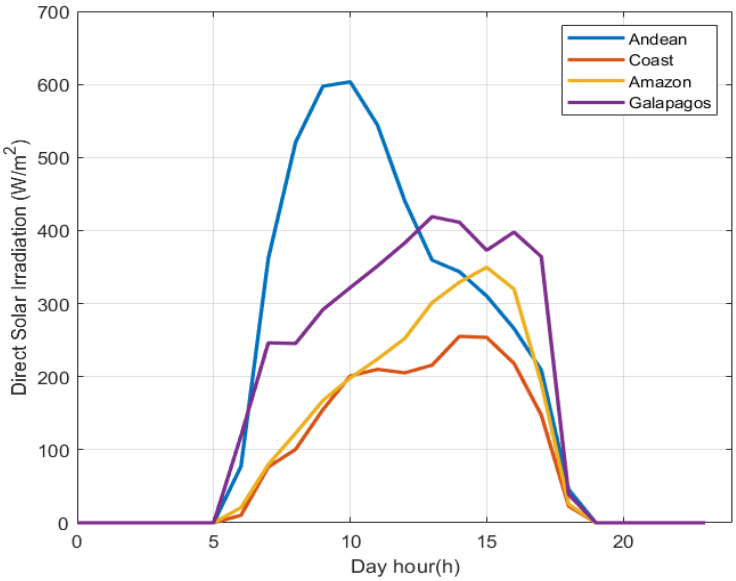

Figure 5. Direct Solar Irradiance (Equator Regions)

Table 2. Thermal Module and ORC Operating Parameters

Parameter	***Symbology***	***Value***	***Reference***
Collector Volume/Area Ratio	***V/Ac***	*8< V/AC<100*	*[33]*
Maximum temperature	$T_{oil,max}$	*300 C*	*[34]*
ΔT of thermal oil	ΔT_{oil}	*50 C*	*[9]*

Heat Loss Coefficient of the Thermal Storage Tank	*uL*	*1 W/m2K*	*[9]*
Turbine isentropic efficiency	$\eta_{is,T}$	*85 %*	*[16]*
Turbine pressure ratio	$\Pi_{T,max}$	*60*	*[9]*
Isentropic pump efficiency	$\eta_{is,b}$	*70 %*	*[16]*
Engine efficiency	η_{motor}	*70 %*	*[9]*
Generator & machine efficiency	η_{mg}	*97 %*	*[35]*
Recuperator Efficiency	η_{Re}	*60 %*	*[16]*
Condensing temperature	T_{cond}	*60 C*	*[9]*
ΔT in the regenerator	ΔT_{sh}	*10 C*	*[36]*
Pinch Point	*PP*	*> 5 C*	*[37]*
Pressure Ratio	*Pmax/Pcrit*	*0.9*	*[35]*

Mathematical model

Table 3 details the equations used to model the thermal modulus and ORC. The thermal modulus and ORC models were solved by applying multi-step implicit methods (Adams-Bashfort) for the initial value problems and by applying the double Newton method. The thermodynamic properties for the ORC calculation were performed with EES-Demo software. The model was developed in MATLAB, taking into account all the thermodynamic properties and analyzing mainly the collector efficiency, the thermodynamic efficiency of the cycle and the total electrical energy produced. On the other hand, the optimization was performed using nonlinear reduced generalized gradient algorithms using the net present value (NPV) as the objective function.

Table 3. Equations used for the system modeling.

Module	***Parameter***	***Equation***
Thermal	*Available Solar Irradiation*	$Q_{solar} = A_c * G_b$
	Useful energy absorbed	$Q_u = m * c_p * (T_{out} - T_{in})$
	Efficiency Solar Collectors	$n_c = \frac{Q_u}{Q_{solar}}$
	Evolution of hot zone temperature (energy storage tank)	$MC_p \frac{\partial T_{St1}}{\partial t} = \dot{m}_c * C_p * (T_{in} - T_{St1}) + \dot{m}_{oil} * C_p * (T_{St2} - T_{St1}) - U_L * A_{St1} * (T_{St1} -$
	Transition zone temperature	$MC_p \frac{\partial T_{St2}}{\partial t} = \dot{m}_c * C_p * (T_{St1} - T_{St2}) + \dot{m}_{oil} * C_p * (T_{St3} - T_{St2}) - U_L * A_{St2} * (T_{St2} -$

	evolution (energy storage tank)	
	Cold zone temperature evolution (Energy storage tank)	$MC_p\frac{\partial T_{St3}}{\partial t} = \dot{m}_c * C_p * (T_{St2} - T_{St3}) + \dot{m}_{oil} * C_p * (T_{oil,out} - T_{St3}) - U_L * A_{St3} * (T_{St}$
	Energy storage tank area	$A_{St1} = \frac{\pi D_{St}^2}{4} + \frac{\pi D_{St} * L_{St}}{3}$ $A_{St2} = \frac{\pi D_{St} * L_{St}}{3}$ $A_{St3} = \frac{\pi D_{St}^2}{4} + \frac{\pi D_{St} * L_{St}}{3}$
ORC	*ORC net work*	$W_{net} = \eta_{mg} * \eta_{orc} * (h_4 - h_5) - \frac{m_{orc} * w_{pump}}{\eta_{mot}}$
	ORC net heat	$Q_{net} = m_{oil} * cp_{oil} * \Delta T_{oil}$
	ORC efficiency	$n_c = \frac{W_{net}}{Q_{net}}$
Thermal - ORC	*Total System Efficiency*	$\eta_{tot} = \frac{E_{el}}{E_{solar}}$ $\eta_{tot} = \eta_c * \eta_{orc} * \eta_{loss}$
	Net present value (NPV)	$VAN = -C_o + \sum_{k=1}^{N} \frac{E_{grid} * K_{el} - K_{O\&M} * C_o}{(1+r)^K}$

3. Results and Discussion

3.1. Model validation

To validate the model, the results were compared with the work developed by Tzivanidis et al. [38]. As Table 4 shows, the calculated percentage errors (%E) are below 3%, indicating the reliability of the modeled process.

Table 4. Model validation

Working Fluid	Parameter	Tzivanidis et al. [38]	Developed Model	Error (%)
Cyclohexane	**T oil inlet ($T_{oil,\ in}$)**	295.6	292.35	0.82%
	Collector Efficiency(η)$_c$	0.6144	0.6322	2.96%
	ORC Efficiency(η)$_c$	0.2536	0.2480	2.91%

3.2. Analysis of Solar Panels

Three (3) analyses were carried out in terms of solar collector performance, taking into account (4) thermal oils (Therminol VP1, Solar Salt, Hitec, Hitec XL) since their thermodynamic properties are an important factor in determining the maximum thermal efficiency of the collectors and the environmental conditions (direct solar radiation and ambient temperature) of the four (4) regions of Ecuador.

3.2.1 Mass Flow Requirement

As shown in Figure 6, the mass flow required varies as a function of the heat capacity of the thermal oil used. The higher the kJ/kgC the oil delivers, the lower the mass flow required to achieve the same ORC cycle power and solar collector performance. Therefore, using oil with better thermodynamic properties significantly reduces the investment for the operation of the thermal module. Table 5 details the characteristics of the thermal oils analyzed and the mass flow required to produce 38 kW of net power (ORC cycle) with a collector efficiency of 50.75%, maintaining the ambient temperature at 14.5 C, direct radiation at 185 W/m2 and using Cyclohexane as the working fluid in the ORC. Based on the analysis, the thermal oil that requires less mass flow to achieve the same performance is Therminol VP1.

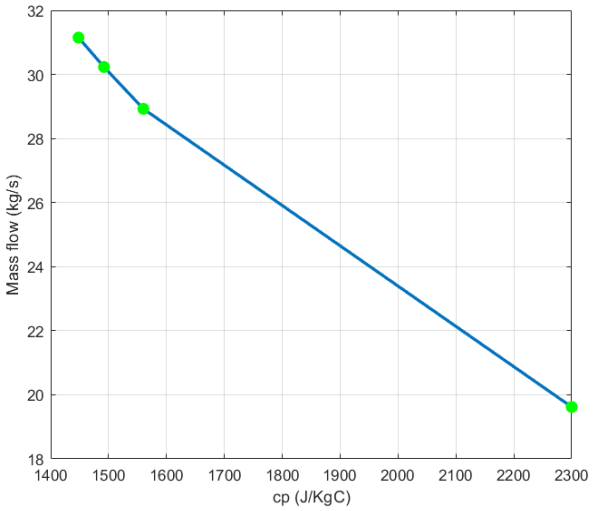

Figure 6. Required mass flow rate as a function of heat capacity of thermal oil

Thermal Oil	Cp (kJ/kgC)	Required mass flow (kg/s)
Therminol VP1	2300	19.62
Hitec	1560	28.92
Molten salts	1492	30.23
Hitec XL	1448	31.15

3.2.2 Collector performance as a function of the oil heat capacity

The collector efficiency was determined as a function of the heat capacity of the oil maintaining a mass flow rate of 19.62 kg/s, and a temperature differential between the inlet and outlet of the

collector of 50 C. As shown in Table 6, the higher the cp of the thermal oil, the higher the efficiency of the solar collector since the efficiency is directly proportional to the heat generated by the solar collector. Therminol VP1 oil provides better operability of the solar collector, achieving an efficiency of approximately 56%. This confirms the findings of [39] that Therminol VP1 is the most suitable oil for solar collector operation since its stability ranges from 12 to 400 C and its thermodynamic efficiency is better than other working fluids such as molten salts and water vapor.

Table 6. Collector performance as a function of thermal oil Cp

Thermal Oil	**Cp (kJ/kgC)**	$\eta_{collector}$
Therminol VP1	2300	0.5540
Hitec	1560	0.3758
Molten salts	1492	0.3594
Hitec XL	1448	0.3498

3.2.3 Collector performance as a function of the amount of direct solar irradiation

The collector performance was calculated as a function of the amount of direct solar irradiation received by the collector and the ambient temperature in each of the regions of Ecuador (Coast, Andean, Amazon and Galapagos). This analysis used the average ambient temperature and direct solar irradiation of a 10-year time series. The Coast region has the highest Tamb (27 C), and the Sierra region has the lowest Tamb (14 C); however, the highest solar radiation levels are found in the Sierra region (194.98 W/m^2). As shown in Table 7, the collectors' efficiency is higher in the Andean Region due to its high level of radiation compared to the other regions. The ideal conditions would be for both (Tamb and Gb) to be higher, but in Ecuador, due to topographic, hydrographic and climatological conditions, it is difficult for these two factors to increase proportionally (Figure 7).

Table 7. Collector performance as a function of Ecuadorian weather conditions

Region	**Tamb (ºC)**	**Gb(W/m)^2**	$\eta_{collector}$
Coast	27.18	86.29	0.3089
Amazon	24.40	107.55	0.3871
Galapagos	21.54	165.12	0.5055
Andean	14.07	194.98	0.5306

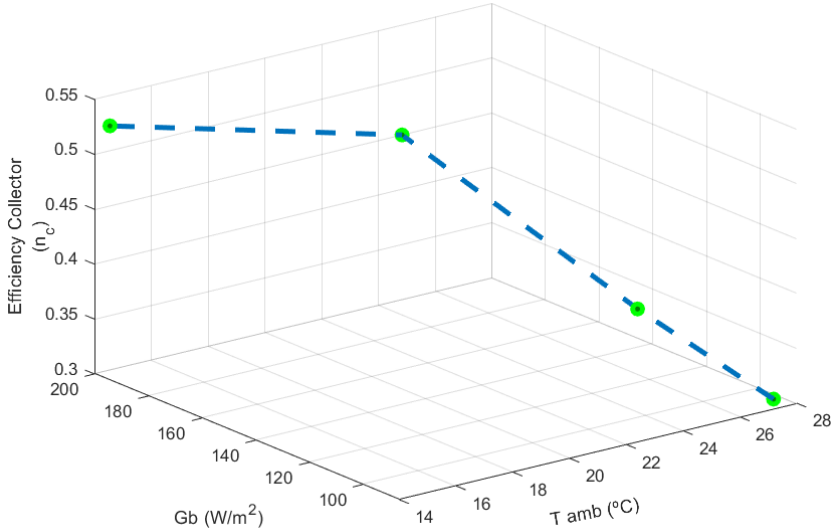

Figure 7. Collector Efficiency as a Function of Ambient Temperature and Solar Radiation

3.3. ORC analysis

3.3.1 Analysis of ORC performance as a function of the evaporation temperature of the working fluid before the turbine inlet

For this analysis, the condensation temperature of the working fluids was kept constant (60 ºC - Toluene and Water, 40 C - Cyclohexane, 87 C - Siloxane D4), and the evaporation temperature (turbine inlet temperature) was varied with a varied range of 210 to 310 C because it is an ORC operated at high temperatures and taking into account the critical temperatures of each fluid. As shown in Figure 8, for all working fluids except Siloxane D-4, the ORC efficiency increases as the boiling temperature increases, and the increase in cycle efficiency for Cyclohexane, toluene, and water are 0.0061%, 0.0046%, and 0.0028% respectively.

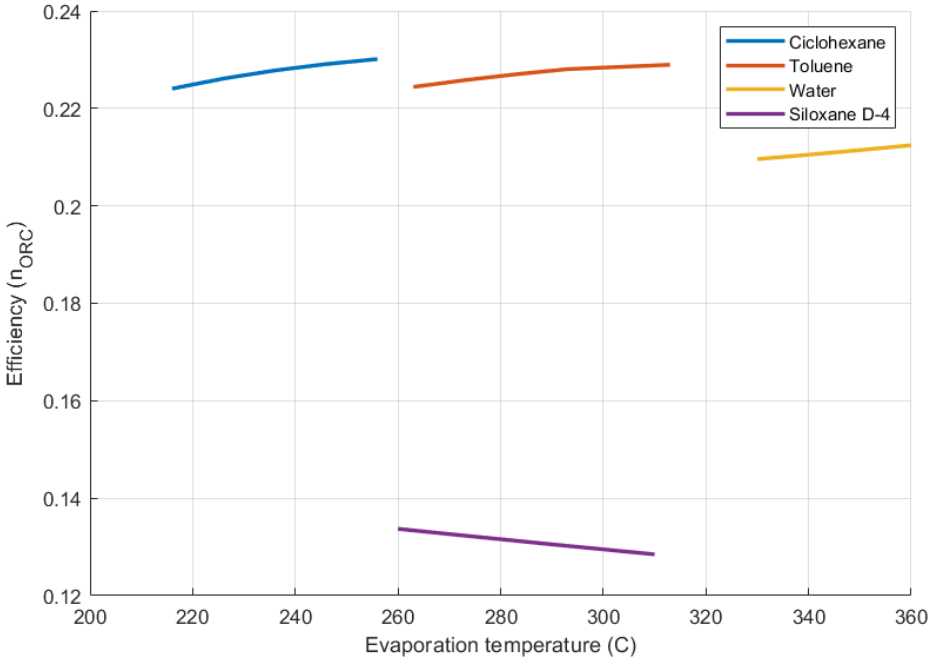

Figure 8. Efficiency of ORC as a function of evaporating temperature.

3.3.2 Analysis of ORC performance as a function of the condensing temperature of the working fluid before the turbine inlet

To perform this analysis, the evaporation temperature of the working fluids was kept constant (302 C - Toluene, 265 C - Cyclohexane, 307 C - Siloxane D4), and the condensation temperature (pump inlet temperature) was varied with a range of variation from 30 to 110 C. As seen in Figure 9, for all working fluids, the ORC efficiency decreases as the condensing temperature increases; however, the decrease in cycle efficiency for toluene, Cyclohexane and Siloxane D4 is 0.014%, 0.0108% and 0.022%, respectively, is minimal.

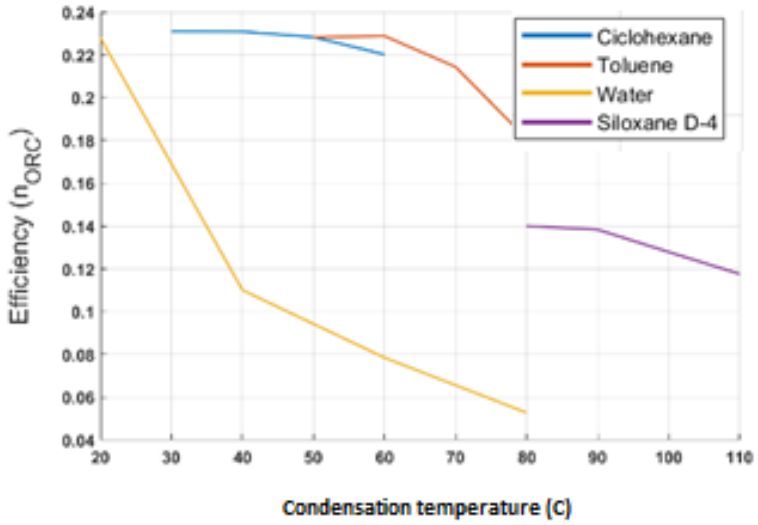

Figure 8. ORC efficiency as a function of condensing temperature.

3.3.3 Analysis of the network the ORC provides as a function of Pinch Point temperature.

According to the results detailed in Table 8, the increase in the pinch point temperature (PP) decreases the net work produced by the system. The choice of the pinch point depends mainly on economic factors since, at a relatively low PP, the heat transfer area increases, and this represents high operating costs; it is for this reason that a variation of the minimum pinch point should be established in such a way that the network production is maximized, but at the same time the system operating costs are minimized. Based on the results, Cyclohexane produces more networks for the temperatures analyzed, resulting in higher ORC performance.

Table 8. Net work varying the pinch point temperature

Working Fluid	**Parameter**	**Pinch Point Temperature (C)**			
		0 C	**10 C**	**20 C**	**30 C**
Cyclohexane	W_{neto}	-	-	379.73	230.61
Toluene		363.99	222.72	160.53	125.54
Water		132.99	111.47	95.97	84.27
Siloxane D4		101.24	78.61	64.27	54.37

3.4. Thermal Modulus Analysis - ORC

3.4.1 Analysis of total system performance as a function of heat transfer area and heat reservoir volume

Figure 9 indicates that for the same operating conditions, the working fluid that induces better total system yields is Cyclohexane, with a maximum yield reaching approximately 25.13% at the most favorable conditions, in contrast to the yields of toluene, water and siloxane D4, which are: 22%, 20.61% and 14.99% respectively.

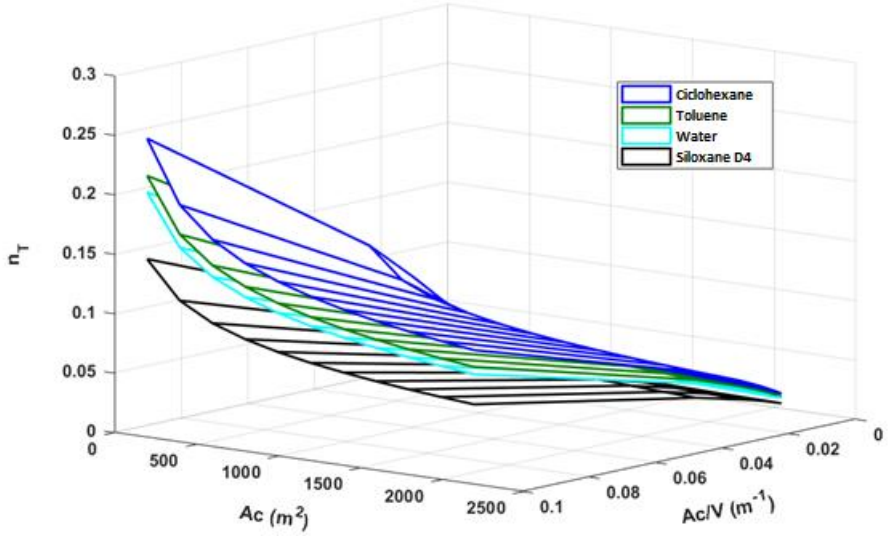

Figure 9. Total system performance as a function of collector area and Ac/V ratio Wnom=f (Collector Area)

3.4.1 Analysis of the network of the system by adding a waste heat source to the ORC

The addition of waste heat to an ORC constitutes an energy cogeneration system, which consists of taking advantage of the exhaust gases of an industrial process (generally cement and sugar

industries) in which the waste heat generated varies in the range of 10 kW to 10 MW [40]. [40]. As shown in Figure 10, when an additional heat source is added (Qresidual = 184 kW) the network of the ORC increases considerably compared to the network performed when the system operates using only the solar collectors as an energy source.

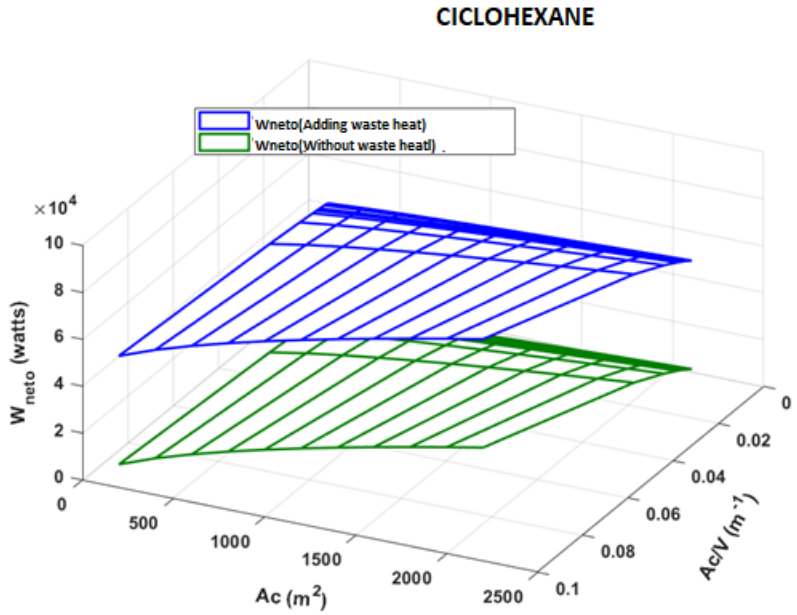

Figure 10. Net work done with solar collectors only and adding a waste heat source.

3.4.2 Internal Rate of Return (IRR) Analysis

As shown in Figure 11a, the IRR increases as the collector area increases, but this increase has a maximum peak (IRR = 15.66%) when the collector area is 1400 to 1650m^2. From that value, the IRR begins to decline, and this effect occurs because the system has been designed to work with a maximum rated power of 92 kW; from 1600 m2, the capacity factor is 100%. Therefore, the increase in the area of the solar collectors does not bring more networks to the system and increases the initial investment costs by increasing the solar collector area exponentially, and for this reason, the growth curve decreases. Similarly, Figure 11b shows that the IRR is practically maintained as the Ac/v ratio increases; however, a maximum peak is observed when the ratio is 0.02 to 0.04 m-1. According to the system optimization, the collector area equals 1600 m^2 with an Ac/v ratio of (1/30) m^{-1}. Once the maximum rate of return has been determined, it is important to determine the minimum payback period to recover the investment and start earning profits. The payback period corresponds to the number of years for which the NPV is minimized. Figure 12 shows the payback period for implementing the system is 9.81 years.

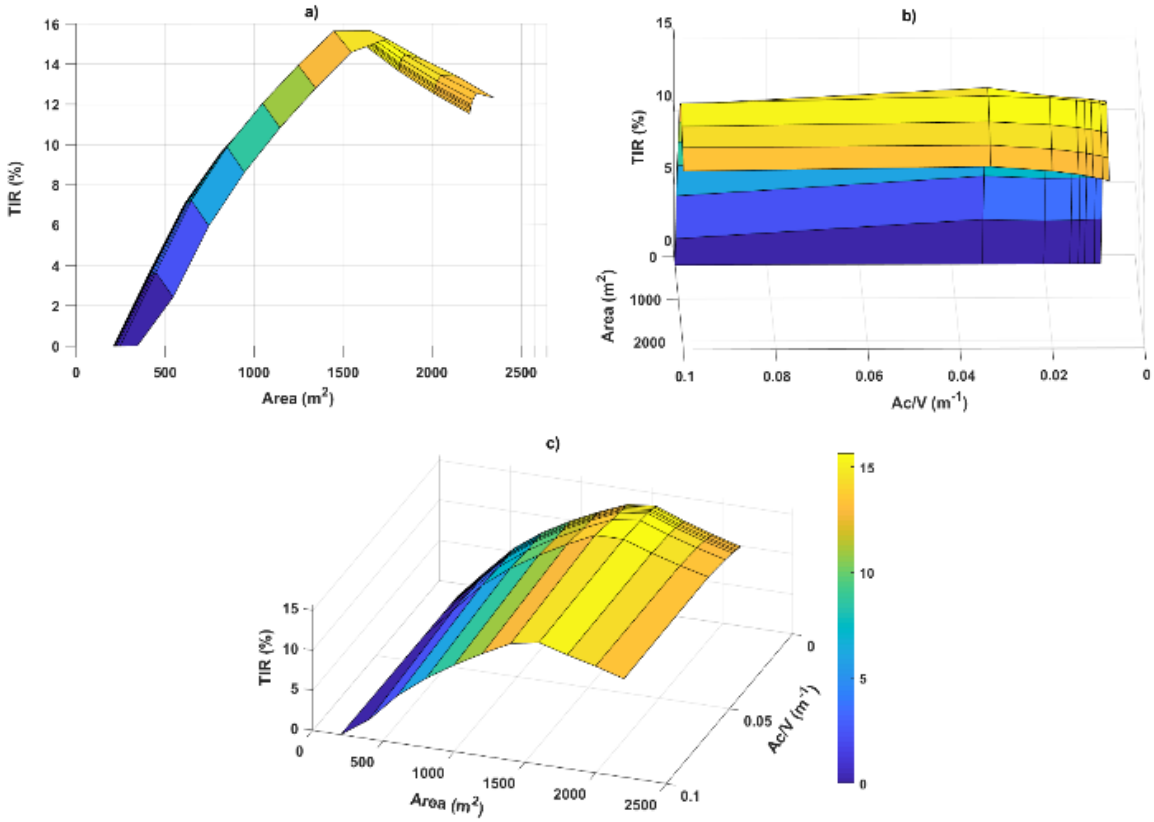

Figure 11. a) Internal rate of return as a function of collector area b) IRR as a function of Ac/V ratio c) IRR as a function of collector area and Ac/V ratio

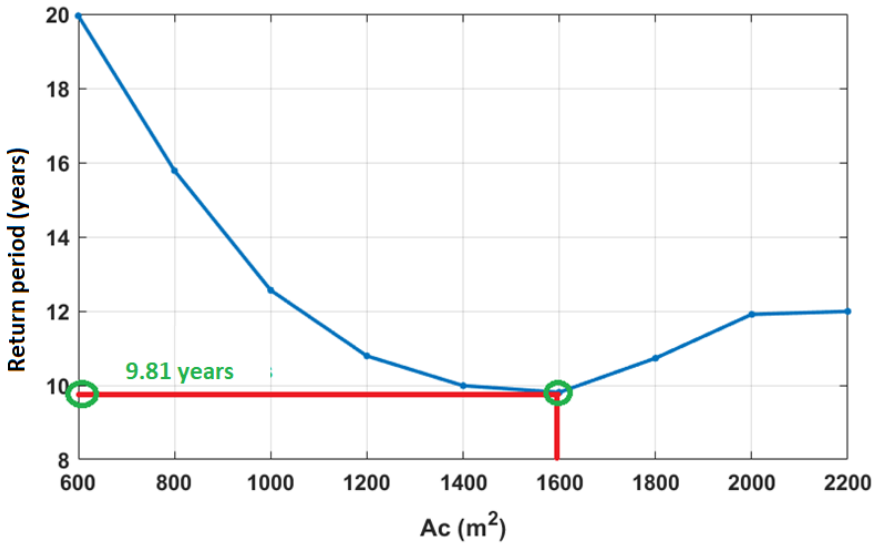

Figure 12. a) Payback period for the initial investment (Ac/V = 30 m-1)

3.5. Optimal operating conditions

Finally, Table 9 summarizes the final results for the optimum operating conditions using Therminol VP1 as the thermal fluid, Cyclohexane as the ORC working fluid, with the meteorological conditions of the Sierra Region of Ecuador and with the Ac and Ac/v ratio that maximize the TIR and minimize the recovery period.

Table 8. Energy parameters of the optimized system.

Parameter	Unit	Value	Parameter	Unit	Value
Collector Area (Ac)	m^2	1600	IRR	%	15.65
Energy reservoir volume (V)	m^3	54	Recovery Period	years	9.81
Oil inlet temperature ($T_{oil,in}$)	C	292.34	Total electric power	TJ	7.42
Collector efficiency $(\eta)_c$	%	50.42 %			
ORC Efficiency $(n)_T$	%	25.01 %			
System Efficiency $(n)_T$	%	20.86 %			

4. Conclusions

An ORC operated with solar collectors was mathematically modeled to evaluate the performance of the thermal module and the ORC by analyzing various operating parameters. The thermal module was analyzed with 4 thermal fluids: Therminol VP1, Hitec, Molten Salts, and Hitec XL. The solar collectors achieved the highest efficiency (55.40%) using Therminol VP1 oil as the thermal fluid. Furthermore, the collectors' efficiency as a function of the meteorological conditions (pressure and temperature) in each of the regions of Ecuador was: 53.06% Sierra, 50.55% Insular, 38.71% Oriente and 30.89% on the Coast. Therefore, it is suggested that implementing a system of this type will have greater operability in both the Sierra and Galapagos regions.

On the other hand, based on the analyses, it can be determined that the ORC performance decreases with increasing temperature since the condensation pressure indirectly increases and the actual work of the pump increases. For the evaporation temperature, the ORC performance is proportional since the higher the temperature, the higher the work of the turbine; however, the temperature cannot exceed the critical temperature of each fluid, which becomes unstable.

Moreover, the ORC efficiency increases with the collector area, and the same effect happens with the Ac/v ratio. For example, for Ac/V = 130-1, with Ac = 200 m2, the network (Wneto) done is 1.45 kW; if the Ac increases 10 times (2000 m2), the Wneto rises to 6.74 kW. Whereas, if the Ac/V increases to 10-1, the Wneto, when Ac = 200 m2, increases considerably to 37.03 kW. However, at higher Ac and Ac/V, the volume of the energy storage tank increases and the system implementation costs become more expensive.

The organic fluid that best suits the operation of the system and that results in obtaining the highest efficiency of the ORC are Cyclohexane; in which if waste heat is added the increase in the rate of electricity production increases considerably, and the percentage increase is approximately 300% in production this percentage varies depending on the area of the collector. Under optimum operating conditions, the network produced increased from 18.30 kW to 65.09 kW.

Finally, the system was optimized, obtaining an IRR of 15.65 % with a payback period of 9.81 years. These results were obtained with a total collector area of 1600 m2 and an energy storage

volume of 54 m3. Therefore, the amount of electricity is estimated at 7.42 TJ per year with a collector, ORC and total efficiency of 50.42%, 25.01% and 20.86%, respectively.

Supplementary Materials: The following are available online at www.mdpi.com/xxx/s1, Figure S1: title, Table S1: title, and Video S1: title.

Author Contributions: Conceptualization, D.CH.V and A.S; methodology, W.D, and D.CH.V ; software, W.D, N.CH.V and J.CH.V; ANN, N.CH.V and J.CH.V; validation, D.CH.V and A.S; formal analysis, D.CH.V and C.C.T; statistical analysis, N.CH.V and J.CH.V, data curation, D.CH.V and A.S.; writing-original draft preparation, D.CH.V and A.S; writing-review and editing, D.CH.V and C.C.T; supervision, C.C.T; funding acquisition, N.CH.V, J.CH.V, D.CH.V. All authors have read and agreed to the published version of the manuscript.

Acknowledgments: The author thanks the Security Research Group on Environment and Engineering, "GISAI" for allowing the execution of this research.

Conflicts of Interest: The authors declare no conflict of interest.

References

1. ARCONEL Balance Nacional de Energia Eléctrica.
2. Ministerio de Electricidad y Energía Renovable *Plan Nacional de Eficiencia Energética 2016-2035*; 2017;
3. Hung, T..; Shai, T..; Wang, S.. A REVIEW OF ORGANIC RANKINE CYCLES (ORCs) FOR THE RECOVERY OF LOW-GRADE WASTE HEAT T. C. **1997**, *22*, 661–667, doi:https://doi.org/10.1016/S0360-5442(96)00165-X.
4. Bao, J.; Zhao, L. A review of working fl uid and expander selections for organic Rankine cycle. *Renew. Sustain. Energy Rev.* **2013**, *24*, 325–342, doi:10.1016/j.rser.2013.03.040.
5. Lecompte, S.; Huisseune, H.; Van Den Broek, M.; Vanslambrouck, B.; De Paepe, M. Review of organic Rankine cycle (ORC) architectures for waste heat recovery. *Renew. Sustain. Energy Rev.* **2015**, *47*, 448–461, doi:10.1016/j.rser.2015.03.089.
6. Vélez, F.; Segovia, J.J.; Martín, M.C.; Antolín, G.; Chejne, F.; Quijano, A. A technical, economical and market review of organic Rankine cycles for the conversion of low-grade heat for power generation. *Renew. Sustain. Energy Rev.* **2012**, *16*, 4175–4189, doi:10.1016/j.rser.2012.03.022.
7. Zhai, H.; An, Q.; Shi, L.; Lemort, V.; Quoilin, S. Categorization and analysis of heat sources for organic Rankine cycle systems. *Renew. Sustain. Energy Rev.* **2016**, *64*, 790–805, doi:10.1016/j.rser.2016.06.076.
8. Karellas, S.; Leontaritis, A.D.; Panousis, G.; Bellos, E.; Kakaras, E. Energetic and exergetic analysis of waste heat recovery systems in the cement industry. *Energy* **2013**, *58*, 147–156, doi:10.1016/j.energy.2013.03.097.
9. Tzivanidis, C.; Bellos, E.; Antonopoulos, K.A. Energetic and financial investigation of a stand-alone solar-thermal Organic Rankine Cycle power plant. *Energy Convers. Manag.* **2016**, *126*, 421–433, doi:10.1016/j.enconman.2016.08.033.
10. Delgado-Torres, A.M.; García-Rodríguez, L. Design recommendations for solar organic Rankine cycle (ORC)-powered reverse osmosis (RO) desalination. *Renew. Sustain. Energy Rev.* **2012**, *16*, 44–53, doi:10.1016/j.rser.2011.07.135.
11. Ferrara, F.; Gimelli, A.; Luongo, A. Small-scale concentrated solar power (CSP) plant: ORCs comparison for different organic fluids. In Proceedings of the 68th Conference of the Italian Thermal Machines Engineering Association, AT12013; Elsevier BV, 2014; Vol. 45,

pp. 217–226.

12. Bianchi, M.; De Pascale, A. Bottoming cycles for electric energy generation: Parametric investigation of available and innovative solutions for the exploitation of low and medium temperature heat sources. *Appl. Energy* **2011**, *88*, 1500–1509, doi:10.1016/j.apenergy.2010.11.013.
13. Sampedro, J.L. Aplicación de Ciclos Rankine orgánico de baja temperatura a sistemas de microgeneración, Universidad de Oviedo, 2017.
14. Borsukiewicz-Gozdur, A.; Nowak, W. Comparative analysis of natural and synthetic refrigerants in application to low temperature Clausius-Rankine cycle. *Energy* **2007**, *32*, 344–352, doi:10.1016/j.energy.2006.07.012.
15. Schuster, A.; Karellas, S.; Kakaras, E.; Spliethoff, H. Energetic and economic investigation of Organic Rankine Cycle applications. *Appl. Therm. Eng.* **2009**, *29*, 1809–1817, doi:10.1016/j.applthermaleng.2008.08.016.
16. Pei, G.; Li, J.; Ji, J. Analysis of low temperature solar thermal electric generation using regenerative Organic Rankine Cycle. *Appl. Therm. Eng.* **2010**, *30*, 998–1004, doi:10.1016/j.applthermaleng.2010.01.011.
17. Chen, Y.; Pridasawas, W.; Lundqvist, P. Low-grade Heat Source Utilization by Carbon Dioxide Transcritical Power Cycle. In Proceedings of the Proceedings of HT2007; Canada, 2017; pp. 1–7.
18. Kane, M.; Larrain, D.; Favrat, D.; Allani, Y. Small hybrid solar power system. *Energy* **2003**, *28*, 1427–1443, doi:10.1016/S0360-5442(03)00127-0.
19. Wang, X.D.; Zhao, L.; Wang, J.L.; Zhang, W.Z.; Zhao, X.Z.; Wu, W. Performance evaluation of a low-temperature solar Rankine cycle system utilizing R245fa. *Sol. Energy* **2010**, *84*, 353–364, doi:10.1016/j.solener.2009.11.004.
20. Al-Sulaiman, F.A. Exergy analysis of parabolic trough solar collectors integrated with combined steam and organic Rankine cycles. *Energy Convers. Manag.* **2014**, *77*, 441–449, doi:10.1016/j.enconman.2013.10.013.
21. Biscan, D.; Filipan, V. Potential of waste heat in croatian industrial sector. *Therm. Sci.* **2012**, *16*, 747–758, doi:10.2298/TSCI120124123B.
22. Tchanche, B.F.; Lambrinos, G.; Frangoudakis, A.; Papadakis, G. Low-grade heat conversion into power using organic Rankine cycles - A review of various applications. *Renew. Sustain. Energy Rev.* **2011**, *15*, 3963–3979, doi:10.1016/j.rser.2011.07.024.
23. Iii, CS; Depcik, C. Review of organic Rankine cycles for internal combustion engine exhaust waste heat recovery. *Appl. Therm. Eng.* **2013**, *51*, 711–722, doi:10.1016/j.applthermaleng.2012.10.017.
24. Xie, H.; Yang, C. Dynamic behavior of Rankine cycle system for waste heat recovery of heavy duty diesel engines under driving cycle. *Appl. Energy* **2013**, *112*, 130–141, doi:10.1016/j.apenergy.2013.05.071.
25. Zhang, H.G.; Wang, E.H.; Fan, BY. A performance analysis of a novel system of a dual loop bottoming organic Rankine cycle (ORC) with a light-duty diesel engine. *Appl. Energy* **2013**, *102*, 1504–1513, doi:10.1016/j.apenergy.2012.09.018.
26. Franco, A.; Villani, M. Geothermics Optimal design of binary cycle power plants for water-dominated , medium-temperature geothermal fields. **2009**, *38*, 379–391, doi:10.1016/j.geothermics.2009.08.001.
27. Zhai, H.; Shi, L.; An, Q. In fl uence of working fl uid properties on system performance and screen evaluation indicators for geothermal ORC (organic Rankine cycle) system. *Energy* **2014**, *74*, 2–11, doi:10.1016/j.energy.2013.12.030.
28. García-Rodríguez, L.; Blanco-Gálvez, J. Solar-heated Rankine cycles for water and

electricity production : POWERSOL project. *Desalination* **2007**, *212*, 311–318, doi:10.1016/j.desal.2006.08.015.

29. Algieri, A.; Morrone, P. Energetic analysis of biomass- fi red ORC systems for micro-scale combined heat and power (CHP) generation . A possible application to the Italian residential sector. *Appl. Therm. Eng.* **2014**, *71*, 751–759, doi:10.1016/j.applthermaleng.2013.11.024.
30. Algieri, A.; Morrone, P. Techno-economic analysis of biomass-fired ORC systems for single-family combined heat and power (CHP) applications. *Energy Procedia* **2014**, *45*, 1285–1294, doi:10.1016/j.egypro.2014.01.134.
31. Drescher, U.; Bru, D. Fluid selection for the Organic Rankine Cycle (ORC) in biomass power and heat plants. **2007**, *27*, 223–228, doi:10.1016/j.applthermaleng.2006.04.024.
32. Bellos, E.; Tzivanidis, C. Parametric investigation of a trigeneration system with an organic Rankine cycle and absorption heat pump driven by parabolic trough collectors for the building sector. *Energies* **2020**, *13*, doi:10.3390/en13071800.
33. Cabrera, F.J.; Fernández-García, A.; Silva, R.M.P.; Pérez-García, M. Use of parabolic trough solar collectors for solar refrigeration and air-conditioning applications. *Renew. Sustain. Energy Rev.* **2013**, *20*, 103–118, doi:10.1016/j.rser.2012.11.081.
34. Chacartegui, R.; Vigna, L.; Becerra, J.A.; Verda, V. Analysis of two heat storage integrations for an Organic Rankine Cycle Parabolic trough solar power plant. *Energy Convers. Manag.* **2016**, *125*, 353–367, doi:10.1016/j.enconman.2016.03.067.
35. Sadeghi, M.; Nemati, A.; ghavimi, A.; Yari, M. Thermodynamic analysis and multi-objective optimization of various ORC (organic Rankine cycle) configurations using zeotropic mixtures. *Energy* **2016**, *109*, 791–802, doi:10.1016/j.energy.2016.05.022.
36. Wang, R.; Jiang, L.; Ma, Z.; Gonzalez-Diaz, A.; Wang, Y.; Roskilly, A.P. Comparative analysis of small-scale organic Rankine cycle systems for solar energy utilisation. *Energies* **2019**, *12*, doi:10.3390/en12050829.
37. Cao, Y.; Gao, Y.; Zheng, Y.; Dai, Y. Optimum design and thermodynamic analysis of a gas turbine and ORC combined cycle with recuperators. *Energy Convers. Manag.* **2016**, *116*, 32–41, doi:10.1016/j.enconman.2016.02.073.
38. Tzivanidis, C.; Bellos, E.; Antonopoulos, K.A. Energetic and financial investigation of a stand-alone solar-thermal Organic Rankine Cycle power plant. *Energy Convers. Manag.* **2016**, *126*, 421–433, doi:10.1016/j.enconman.2016.08.033.
39. Krishna, Y.; Faizal, M.; Saidur, R.; Ng, K.C.; Aslfattahi, N. State-of-the-art heat transfer fluids for parabolic trough collector. *Int. J. Heat Mass Transf.* **2020**, *152*, doi:10.1016/j.ijheatmasstransfer.2020.119541.
40. Haunreiter, B. Estudio de las alternativas técnicas y económicas para la recuperación de calor residual en la Termoeléctrica Quevedo II tomando en cuenta aspectos de mitigación de cambio climático, Escuela Politécnica Nacional, 2017.